

Superentropic AdS Black Hole Shadows

A. Belhaj ^{*}, H. Belmahi [†], M. Benali ^{‡§}

Département de Physique, Equipe des Sciences de la matière et du rayonnement, ESMaR

Faculté des Sciences, Université Mohammed V de Rabat, Rabat, Morocco

October 14, 2021

Abstract

We study shadow aspects of superentropic black holes in four dimensions. Using Hamilton-Jacobi formalism, we first get the null geodesic equations. In the celestial coordinate framework relying on fixed positions of observers, we investigate the shadow behaviors in terms of the mass and the cosmological scale variation parameters. Among others, we obtain ellipse shaped geometries contrary to usual black hole solutions. Modifying the ordinary relations describing geometrical observables, we discuss the size and the shape deformation parameters of these non-trivial geometric forms. Due to horizonless limits associated with certain mass values, we explore the shadow of the naked singularity of such black holes.

Keywords: Superentropic, Cosmological constant, Shadows, Geometrical observables.

^{*}a-belhaj@um5r.ac.ma

[†]hajar_belmahi@um5.ac.ma

[‡]mohamed_benali4@um5.ac.ma

[§]Authors in alphabetical order.

Contents

1	Introduction	2
2	Superentropic black hole models	3
3	Geodesic equations of motion	4
4	Shadow behaviors	5
4.1	Shadows of existing horizons	5
4.2	Geometric observables	8
4.3	Naked singularity	10
5	Conclusion	12

1 Introduction

Recently, there has been a great interest in black hole physics in connection with various gravity theories. This has been encouraged by remarkable efforts of Event Horizon Telescope collaborations. These international activities have provided interesting imaging of supermassive black holes at the center of galaxy 87 [1–3]. Remarkably, various works have dealt with thermodynamic and optical aspects of such fascinating objects. In Anti-de Sitter (AdS) geometries, non-trivial results associated with many transitions in black holes have been approached [4, 5]. In particular, the Hawking-Page transition has been investigated in different backgrounds including string-theory and related models [6, 7]. It has been shown that the study of such a transition unveil certain universalities reported in [8, 9]. Parallely to these efforts, optical behaviors have been investigated by considering the deflection angle of lights and the shadow geometry [10–16]. Concretely, the black hole shadow behaviors have been examined in different theories including M-theory and superstring theory in the presence of D-brane objects [17, 18]. The visualization of the shadow cast using the null geodesic equations has been completed by the study of geometrical observables. These quantities provide information about the involved size and the shape. For non-rotating black holes, it has been revealed that the shadow has a circular geometry where its size can be controlled by the mass and other parameters including the charge and dark energy [19]. This geometric manifestation is distorted for ordinary rotating black holes, to exhibit either the D-shape or the cardioid geometries [17, 18, 20, 21]. In addition, it has been shown that the shadow behaviors depend also on other parameters including the brane number and a cosmological scale [18, 22].

More recently, several efforts have been devoted to explore and study the pulsar SGR J174-2900 near supermassive black holes SgrA* [23]. This provides data on the horizon and the

horizonless of events around such compact objects. It has been shown that for rotating black holes or a naked singularity, the emission frequency of such a pulsar could be modified [24]. A special interest has been put on superentropic black holes as a fascinate solution with non compact horizon topologies which could exceed entropy of maximum bounds [25, 26]. Imposing appropriate limits, the superentropic black hole is considered as an ultraspinning limit of the Kerr-Newman-AdS solution [27, 28]. Many investigations have been conducted by approaching such a class of black holes. More precisely, the thermodynamic aspects have been studied in [29, 30]. In particular, it has been established an interplay between the thermodynamics of these black holes and the usual ones using the ultra-spinning approximation limits [30, 31]. Moreover, it has been shown that the superentropic version of certain usual black holes cannot be derived from ultra-spinning ones [32, 33].

The aim of this work is to contribute to these activities by investigating shadow aspects of superentropic black holes in four dimensions. Concretely, we first derive the associated null geodesic equations of motion using the Hamilton-Jacobi formalism. Fixing the observer positions, we then obtain the celestial coordinates needed to illustrate the corresponding shadow behaviors by varying the mass and the cosmological scale parameters. Among others, we find elliptic shaped geometries contrary to usual black holes. Modifying the ordinary relations describing geometrical observables, we study the size and the shape deformation parameters of the obtained non-trivial geometric forms. Due to horizonless limits for certain mass values, we explore the shadow of naked singularity of such black hole solutions.

The organization of this work is follows. In section 2, we give a concise review on superentropic black hole solutions. In section 3, we elaborate the associated geodesic photon equations using the Hamilton-Jacobi analysis. In section 4, we investigate the shadow behaviors. The last section is devoted to conclusions and open questions.

2 Superentropic black hole models

In this section, we give a concise review on of superentropic black hole models in four dimensions, being new solutions of the Einstien-Maxwell equations. These solutions could be obtained from Kerr-Newman- AdS_4 black holes where the rotating parameter is replaced by the AdS length scale using an appropriate approximation limit [28]. According to [30, 31], the line element of the associated metric reads as

$$\begin{aligned}
 ds^2 = & - \frac{\Delta_r}{\Sigma} (dt - \ell \sin^2 \theta d\phi)^2 + \Sigma \left(\frac{dr^2}{\Delta_r} + \frac{d\theta^2}{\sin^2 \theta} \right) \\
 & + \frac{\sin^4 \theta}{\Sigma} (\ell dt - (r^2 + \ell^2) d\phi)^2,
 \end{aligned} \tag{2.1}$$

where ℓ is the AdS radius length being connected to the cosmological constant Λ via the relation

$$\Lambda = -\frac{3}{\ell^2}. \tag{2.2}$$

The involved quantities are expressed as follows

$$\Sigma = r^2 + \ell^2 \cos^2 \theta, \quad \Delta_r = \left(\ell + \frac{r^2}{\ell}\right)^2 - 2mr + q^2. \quad (2.3)$$

It is noted that m and q are the mass and the charge parameters, respectively. The local coordinate ϕ , being a noncompact direction, should be compactified as follows $\phi \sim \phi + \alpha$, where α is a dimensionless parameter. The later has been identified with a new chemical potential K [31]. Solving the equation $\Delta_r = 0$, one can get the large root r_+ , corresponding to the existence of the black hole horizon. Such a solution requires a constraint on the mass parameter given by

$$m \geq 2r_c \left(\frac{r_c^2}{\ell^2} + 1\right), \quad (2.4)$$

where one has $r_c^2 = \frac{\ell^2}{3} \left[\left(4 + \frac{3}{\ell^2} q^2\right)^{1/2} - 1 \right]$. This constraint being a relationship between m , ℓ and q black hole parameters provides two kinds of superentropic black hole solutions. Precisely, the first one is associated with the existence of the horizon, where the constraint is verified. However, the second one corresponds to a naked singularity where Δ_r takes complex values. In this way, the range of parameters are reduced up to such a constraint. The thermodynamics of such black hole solutions have been investigated in many places including in [30]. In particular, certain quantities have been approached in terms of usual charged and rotating black holes. Here, however, we attempt to unveil the associated optical behaviors. Concretely, we study the shadow geometric forms casted by ultra-spinning black holes in four dimensions.

3 Geodesic equations of motion

Before presenting shadow aspects, we first elaborate the geodesic equations of motion using test particles. In particular, the equations of photons surrounding the black hole horizons can be obtained by exploiting the Hamilton-Jacobi formalism. According to [34], one uses the following relation

$$\frac{\partial S}{\partial \tau} + \frac{1}{2} g^{\mu\nu} \frac{\partial S}{\partial x^\mu} \frac{\partial S}{\partial x^\nu} = 0, \quad (3.1)$$

where τ is the affine parameter satisfying the geodesic equations, and where $g_{\mu\nu}$ is the associated metric. S denotes the Jacobi action which reads as

$$S = -Et + L\phi + S_r(r) + S_\theta(\theta), \quad (3.2)$$

where E and L are the total energy and the angular momentum of the photons, respectively. They are related to the four-momentum p_μ via the relations $E = -p_t$ and $L = p_\phi$. It is noted that $S_r(r)$ and $S_\theta(\theta)$ are two functions depending on r and θ variables, respectively. Implementing the separation method and the Carter constant, the complete null geodesic equations can be given in terms of the impact parameters expressed as follows

$$\xi = \frac{L}{E}, \quad \eta = \frac{\mathcal{K}}{E^2}, \quad (3.3)$$

where \mathcal{K} is a separable constant [35]. To get the desired relations, certain computations should be performed. Indeed, they generate the following null geodesic equations

$$\Sigma \frac{dt}{d\tau} = E \left[\frac{A(r^2 + \ell^2)}{\Delta_r} + \frac{\ell(\xi - \ell \sin^2 \theta)}{\sin^2 \theta} \right], \quad (3.4)$$

$$\Sigma \frac{dr}{d\tau} = \sqrt{\mathcal{R}(r)}, \quad (3.5)$$

$$\Sigma \frac{d\theta}{d\tau} = \sqrt{\Theta(\theta)}, \quad (3.6)$$

$$\Sigma \frac{d\phi}{d\tau} = E \left[\frac{A\ell}{\Delta_r} + \frac{\xi - \ell \sin^2 \theta}{\sin^4 \theta} \right], \quad (3.7)$$

where the radial $\mathcal{R}(r)$ and the polar $\Theta(\theta)$ functions of motion are given by

$$\mathcal{R}(r) = E^2 [A^2 - \Delta_r ((\ell - \xi)^2 + \eta)], \quad (3.8)$$

$$\Theta(\theta) = E^2 [\eta \sin^2 \theta - \cos^2 \theta (\xi^2 \cos^2 \theta - 2\xi)], \quad (3.9)$$

and where one has taken $A = (r^2 + \ell^2) - \ell\xi$.

4 Shadow behaviors

In this section, we study the shadow aspects of superentropic black holes. First, we consider the existing horizons. Then, we deal with the naked singularity behaviors associated with non-existing horizons.

4.1 Shadows of existing horizons

For this situation, the boundary of the black hole geometric shapes can be determined from the unstable circular orbits characterized by

$$\mathcal{R}(r) \Big|_{r=r_s} = \frac{d\mathcal{R}(r)}{dr} \Big|_{r=r_s} = 0, \quad (4.1)$$

where r_s is the circular orbit radius of the photon [16]. Appropriate performed calculations give

$$\eta = \frac{r^2 (16\ell^2 \Delta_r - (4\Delta_r - r\Delta_r')^2)}{\ell^2 \Delta_r'^2} \Big|_{r=r_s}, \quad (4.2)$$

$$\xi = \frac{(r^2 + \ell^2) \Delta_r' - 4r\Delta_r}{\ell \Delta_r'} \Big|_{r=r_s}. \quad (4.3)$$

It is known, in the presence of the cosmological constant, that the distance r_{ob} of the observer in domain of outer communications ($\Delta_r > 0$) should be fixed [36, 37]. To get shadow

geometries of the superentropic AdS black holes, we assume that the observer is located in the following frame

$$e_0 = \frac{(r^2 + \ell^2)\partial_t + \ell\partial_\phi}{\sqrt{\Delta_r\Sigma}} \Big|_{(r_{ob}, \theta_{ob})}, \quad (4.4)$$

$$e_1 = \frac{\sin\theta}{\sqrt{\Sigma}}\partial_\theta \Big|_{(r_{ob}, \theta_{ob})}, \quad (4.5)$$

$$e_2 = -\frac{\ell\sin^2\theta\partial_t + \partial_\phi}{\sqrt{\Sigma}\sin^2\theta} \Big|_{(r_{ob}, \theta_{ob})}, \quad (4.6)$$

$$e_3 = -\frac{\sqrt{\Delta_r}}{\sqrt{\Sigma}}\partial_r \Big|_{(r_{ob}, \theta_{ob})}. \quad (4.7)$$

The timelike vector e_0 represents the four-velocity of the observer. e_3 indicates the vector along the spatial direction pointing toward the center of the black hole. However, $e_0 \pm e_3$ can be considered as tangent directions to the one of principal null congruences and θ_{ob} is the angle of the observer. In particular, we consider the ray of lights being characterized by the equation $\lambda(s) = (r(s), \theta(s), \phi(s), t(s))$ and tangent to the observer position

$$\dot{\lambda} = \dot{r}\partial_r + \dot{\theta}\partial_\theta + \dot{\phi}\partial_\phi + \dot{t}\partial_t, \quad (4.8)$$

where the 3-vector of the spacelike can be represented in a basis corresponding to the spherical coordinates. Introducing such coordinates, we get the tangent equation in terms of orthonormal tetrads and celestial coordinates as follows

$$\dot{\lambda} = \beta(-e_0 + \sin\psi\cos\delta e_1 + \sin\psi\sin\delta e_2 + \cos\psi e_3), \quad (4.9)$$

where β is a scalar factor [37, 38]. Combining the ray of light equations and Eq.(4.9), we obtain

$$\beta = g(\dot{\lambda}, e_0) = \frac{E}{\sqrt{\Delta_r\Sigma}} \left(\ell\xi - (r^2 + \ell^2) \right) \Big|_{(r_{ob}, \theta_{ob})}. \quad (4.10)$$

An examination reveals that the celestial coordinates ψ and δ can be expressed as a function of the impact parameters ξ and η . The comparison of the coefficients ∂_r and ∂_ϕ gives the celestial coordinates in the terms of \dot{r} and $\dot{\phi}$. Exploiting Eq.(3.5) and Eq.(3.7), we get the celestial coordinates as a function of ξ and η

$$\sin\psi = \frac{\pm\sqrt{\Delta_r}\eta}{((r^2 + \ell^2) - \ell\xi)} \Big|_{(r_{ob}, \theta_{ob})}, \quad (4.11)$$

$$\sin\delta = \frac{\sqrt{\Delta_r}}{\sin\psi} \left(\frac{(\ell - \csc^2\theta\xi)}{\ell\xi - (r^2 + \ell^2)} \right) \Big|_{(r_{ob}, \theta_{ob})}. \quad (4.12)$$

According to [38], the boundary of the shadows can be obtained using the cartesian coordinate system

$$x = -2 \tan\left(\frac{\psi}{2}\right) \sin\delta, \quad (4.13)$$

$$y = -2 \tan\left(\frac{\psi}{2}\right) \cos\delta. \quad (4.14)$$

A close inspection shows that the shadow behaviors depend on certain black hole parameters including the mass, the charge and the cosmological scale. To visualize such geometric configurations, we first consider neutral solutions. In Fig.(1), the corresponding shadow aspects are plotted in such a plane by exploiting x and y expressions. Concretely, we illustrate

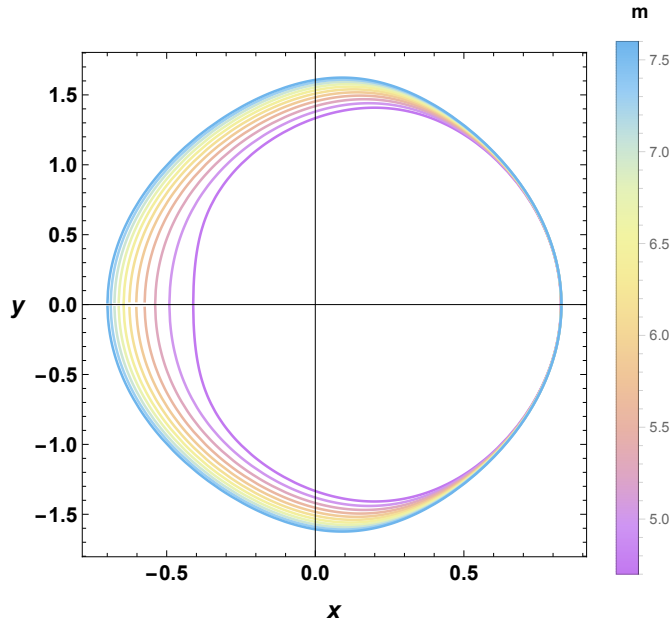


Figure 1: *Shadow behaviors of superentropic AdS black holes for different values of m in the horizon domain existence, by taking $\ell = 3$ and $q = 0$. The observer is positioned at $r_{ob} = 100$ and $\theta_{ob} = \frac{\pi}{2}$*

the shadow geometrical behaviors in terms of the parameter m of the reduced moduli space associated with the existence of the horizon. It follows from this figure that the shadow ellipse shaped geometry is increased by increasing the mass parameter m . For the values of m close to a critical mass $m_c = 2r_c(r_c^2/\ell^2 + 1)$, we obtain the D-shape elliptic geometry. For the values of m above to such a critical mass, the D-shape elliptic geometry disappears. This shadow behavior comes from the black hole mass variation. The latter is associated with the horizon existence as functions of black hole parameters including ℓ , m and q . It has been remarked that the geometry of the shadow is not a perfect circle arising in ordinary non-rotating black holes [39–43].

Having discussed the effect of the mass parameter on non-charged black holes, we move now to introduce the influence of the ℓ parameter on the shadow geometry. Fixing the mass parameter to the value $m = 15.4$ associated with $\ell = 10$, we illustrate the corresponding behaviors by varying ℓ . An examination of Eq.(2.2) shows that one can consider the range $3 \leq \ell \leq 10$ to keep the AdS solutions. This computation is depicted in Fig.(2). It is observed, from this figure, that the shadow geometry size is increased by decreasing the parameter ℓ . For the values of the parameter ℓ close to the value $\ell = 10$, we recover the

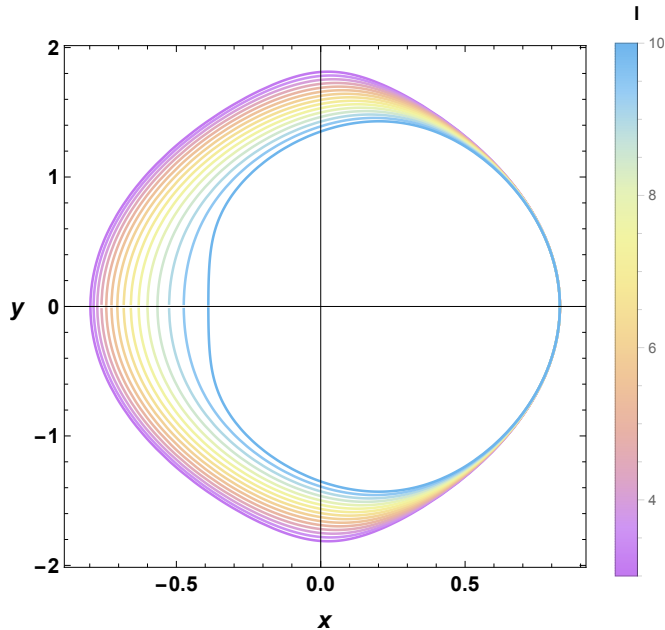


Figure 2: *Shadow behaviors of superentropic AdS black holes for different values of ℓ , by taking $m = 15.4$ and $q = 0$. The observer is located at $r_{ob} = 100$ and $\theta_{ob} = \frac{\pi}{2}$.*

D-shape elliptic geometry. For $3 \leq \ell \leq 9$, however, we obtain a generic ellipse shaped configuration. Fixing the mass parameter, it has been remarked that the large values of the ℓ parameter, associated with D-shape geometry, can play the same role as the rotating one of ordinary black hole solutions. Now, we inspect the charge influence on such geometries by fixing m and ℓ . The variation of the shadow behaviors in terms of the charge parameter q is represented in Fig.(3). For $0 \leq q \leq 1$, it has been remarked that the shadow geometry involves the same shape. This could suggest that the charge does not involve relevant effects.

4.2 Geometric observables

Here, we discuss the geometrical observables controlling the size and the shape of the studied shadows. A close examination shows that the usual relations could be modified due to elliptic geometry of shadows. A priori, there could be many ways to do so. However, we consider here a simple calculation. In this way, one has the radius R_c , which represents the maximal radius of the ellipse shaped geometry, and the distortion D_c indicating the distance between the no-deformed ellipse and the D-shaped one. Following [44, 45], the shadow of the black hole is characterized by three specific points. However, the positions of the top (x_t, y_t) and the bottom (x_b, y_b) positions have been modified according to the present case. The point of a standard ellipse $(\tilde{x}_p, 0)$ and the point of the distorted shadow ellipse $(x_p, 0)$ intersect the horizontal axis associated with the x direction. This modification is illustrated in Fig.(4). It

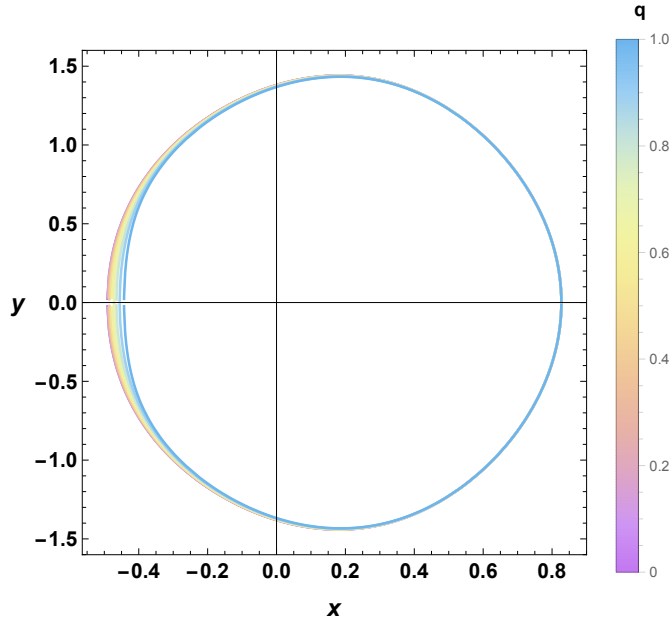


Figure 3: *Shadow behaviors of superentropic AdS black holes for different values of q , by taking $m = 5$ and $\ell = 3$. The observer is positioned at $r_{ob} = 100$ and $\theta_{ob} = \frac{\pi}{2}$.*

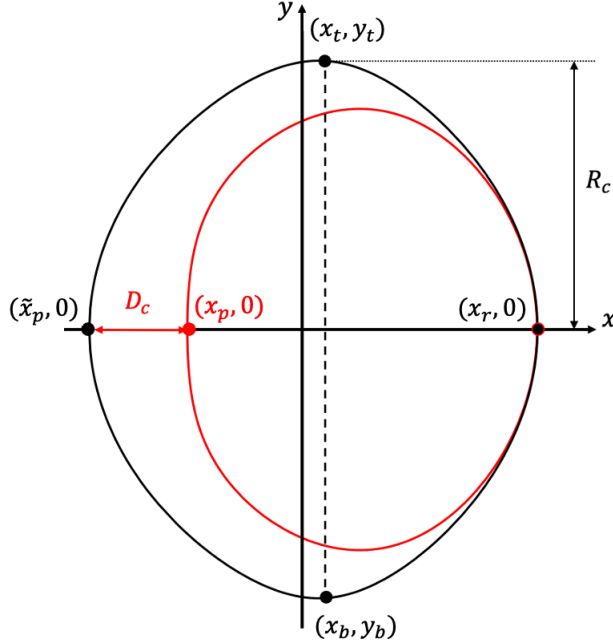


Figure 4: *Illustration of parameter deformations of shadows.*

is worth noting that the usual relations can be recovered by taking the circular limit. Now, we discuss such modified geometrical quantities. The associated computations are given in Fig.(5) and Fig(6). Varying the mass parameter, the R_c behavior has been illustrated for various values of ℓ . It has been observed from Fig.(5) that such a parameter increases in

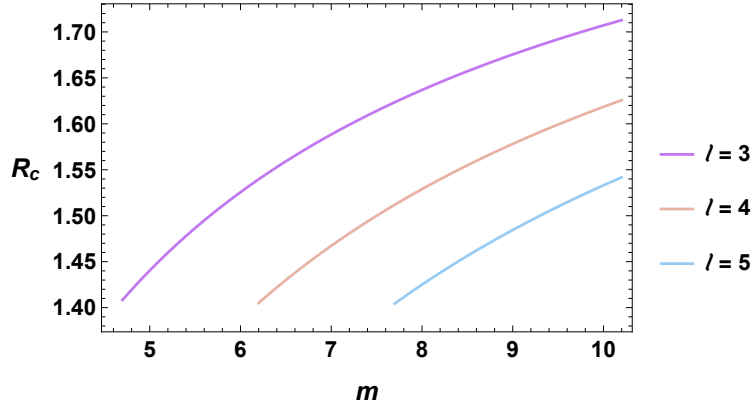


Figure 5: *Size variations of superentropic AdS black holes for different values of m , and ℓ by taking $q = 0$.*

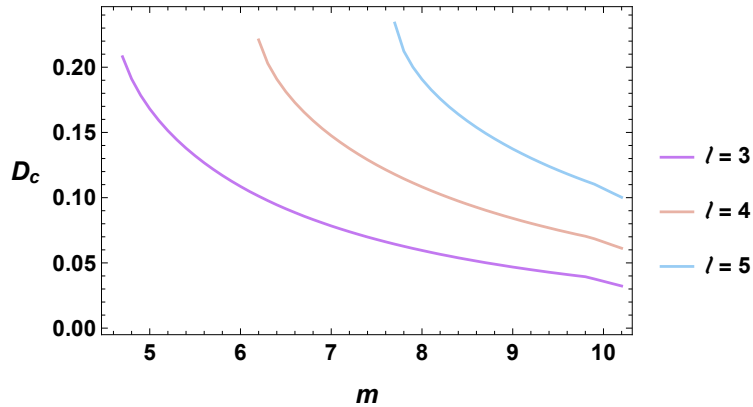


Figure 6: *Shape deformations of superentropic AdS black holes for different values of m , and ℓ by taking $q = 0$.*

terms of m . At generic values of this parameter, R_c decreases with the cosmological scale ℓ . Fig.(6) shows the behavior of D_c in terms of m . It follows from this figure that D_c decreases by increasing m . Contrary to R_c , D_c increases with ℓ for fixed values of m .

4.3 Naked singularity

It has been shown that black holes and naked singularities can be distinguished using different approaches including accretion disks [46]. We expect that the shadow geometric configuration can be also exploited to show such distinctions. In the vicinity of naked singularities, it has been suggested that gravity effects should be dominant, which could be visible from the shadow geometric configurations. In this way, this new optical characteristic of such a singularity can also be exploited to unveil more data in the future shadow observations of the galactic center M87 [2]. For such reasons, we discuss the naked singularity shadows of superentropic AdS black holes in four dimensions. Inspecting the previous shadow geome-

tries, the unstable spherical orbits of the photons involve an elliptic geometry. In the naked singularity, however, such orbits are illustrated by arcs. It is recalled that the naked singularity appears when the largest root of $\Delta_r = 0$ takes complex values. Due to the horizon absence for certain values of the mass lower to the critical mass of the superentropic AdS black holes, the photons which are close to both sides of the possible arcs can be seen by the observer [47, 48].

Considering neutral solutions and taking into account the critical mass constraint, we vary the cosmological parameter ℓ with the same range of the mass parameter in the domain of the horizonless. In this way, one should have $m < m_c$ for generic values of ℓ . In Fig.(7),

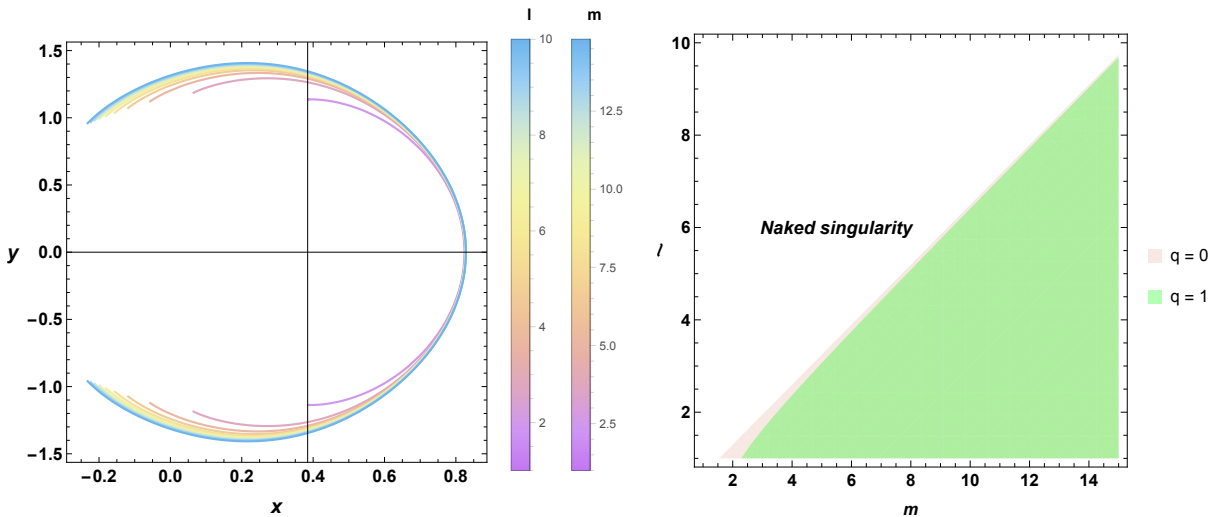


Figure 7: Left the shadow behaviors of superentropic AdS black holes for different values of m , and ℓ by taking $q = 0$, the right the region plot for the superentropic AdS black holes as function of parameters l , m and q . The observer is positioned at $r_{ob} = 100$ and $\theta_{ob} = \frac{\pi}{2}$.

we illustrate the naked singularity behaviors for non-charged solutions by varying the mass parameter in appropriate range of ℓ . It is observed that the length of the arcs depends on such parameter variations. In particular, it is increasing with m and ℓ . It has been observed that the arcs became closed when the m and ℓ black hole parameters increase. This could be understood from the mass variation. In Fig.(7), we plot the horizon region and the naked singularity for such a black hole as a function of the parameters m and ℓ for certain specific values of q . In the absence of the charge, the horizon region is relevant with respect to charged solutions. It has been remarked that generic values of $q > 1$, the difference is significant.

5 Conclusion

In this work, we have investigated shadow behaviors of superentropic black holes in four dimensions. It has been shown that the mass constraint have generated two different solutions associated with superentropic black holes, being existing horizons and naked singularities. Applying the Hamilton-Jacobi method, we have first found the null geodesic equations. In the celestial coordinate framework associated with fixed positions of observers, we have engineered the shadow geometries of existing horizons by varying the mass and the cosmological scale parameters. Among others, the size shadow augments with the mass. However, it decreases with the cosmological scale length. Concretely, we have obtained ellipse shaped geometries contrary to usual black hole solutions. For fixed values of ℓ , the ellipse D-shape geometry appears for particular mass values. This result could be supported by the fact that such black holes, with the mass constraint, involve a fast spinning motion. Modifying the ordinary relations describing geometrical observables, we have examined the size and the distortion parameters of such elliptic forms. To make a distinction between such two possible solutions, we have investigated the geometrical behavior of the shadow associated with the horizon-less configuration. In this way, the shadow geometries have been given in terms of arcs depending on black holes physical parameters. The size of these arcs increases with the mass and the AdS radius. It has been observed that these parameters act on such geometrical configurations in a similar way.

This work comes up with certain questions. A natural question concerns higher dimensional solutions which could be dealt with in alternative theories including stringy models. Such a subject could open new roads to unveil significant physical data on rotating black hole physics. Precisely, this could bring new candidate geometries to model realistic black holes in four dimensions. It should be interesting to implement new physical aspects to study distinctions between horizon existing and horizon-less solutions. We believe that these observations deeper reflections. These left for future works.

Acknowledgements

The authors would like to thank A. El Balali, W. El Hadri, H. El Moumni, Y. Hassouni, M. B. Sedra, Y. Sekhmani, M. Oulaid, E. Torrente Lujano for discussions on related topics and correspondence. MB would like to thank Di Wu for emailing discussions about the present work. This work is partially supported by the ICTP through AF.

References

- [1] K. Akiyama and al., *First M87 Event Horizon Telescope Results. IV. Imaging the Central Supermassive Black Hole*, *Astrophys. J.* **L4** (1) (2019) 875, [arXiv:1906.11241](#).

- [2] K. Akiyama and al., *First M87 Event Horizon Telescope Results. V. Imaging the Central Supermassive Black Hole*, *Astrophys. J.* **L5** (1) (2019) 875.
- [3] K. Akiyama and al., *First M87 Event Horizon Telescope Results. VI. Imaging the Central Supermassive Black Hole*, *Astrophys. J.* **L6** (1) (2019) 875.
- [4] S. W. Hawking and D. N. Page, *Thermodynamics of black holes in anti-de Sitter space*, *Commun. Math. Phys.* **87** (4) (1983) 577.
- [5] D. Kubizňák, R. B. Mann and Mae Teo, *Black hole chemistry: thermodynamics with Lambda*, *Class. Quantum Grav.* **34** (2017) 06300, [arXiv:1608.06147](#).
- [6] Y-Y. Wang, B-Y Su and N. Li, *Hawking Page phase transitions in four-dimensional Einstein Gauss Bonnet gravity*, *Phys. Dark Universe* **31** (2021) 100769, [arXiv:2008.01985](#).
- [7] A. Buchel, L. A. Pando Zayas, *Hagedorn versus Hawking-Page transition in string theory*, *Phys.Rev. D* **68** (2003) 066012, [arXiv:hep-th/0305179](#).
- [8] A. Belhaj, A. El Balali, W. El Hadri, E. Torrente-Lujan, *On Universal Constants of AdS Black Holes from Hawking-Page Phase Transition*, *Physics Letters B* **811**(2020) 135871, [arXiv:2010.07837](#).
- [9] S.W. Wei, Y.X. Liu, R.B. Mann and R. B. Mann, *Novel dual relation and constant in Hawking-Page phase transitions*, *Phys.Rev. D* **102** (08)(2020) 104011, [arXiv:2006.11503](#).
- [10] S. W. Wei, Y. C. Zou, Y. X. Liu and R. B. Mann, *Curvature radius and Kerr black hole shadow*, *JCAP* **08** (2019) 030, [arXiv:1904.07710](#).
- [11] A. Övgün, I. Sakalli and J. Saavedra, *Shadow cast and Deflection angle of Kerr-Newman-Kasuya spacetime*, *JCAP.* **10** (2018) 041, [arXiv:1807.00388](#).
- [12] R. Uniyal, H. Nandan and P. Jetzer, *Bending angle of light in equatorial plane of Kerr-Sen Black Hole*, *Phys. Lett. B* **782** (2018) 185, [arXiv:1803.04268](#) .
- [13] P. Sharma, H. Nandan, R. Gannouji, R. Uniyal and A. Abebe, *Deflection of light by a rotating black hole surrounded by quintessence* , *Int. J. Mod. Phys. A* **35** (2020) 2050155, [arXiv:1911.00372](#).
- [14] A. Övgün, İ. Sakallı and J. Saavedra, *Shadow cast and Deflection angle of Kerr-Newman-Kasuya spacetime*, *JCAP* **10** (2018) 041,[arXiv:1807.00388](#).
- [15] X. Hou, Z. Xu and J. Wang, *Rotating black hole shadow in perfect fluid dark matter*, *JCAP* **12** (2018) 040,[arXiv:1810.06381](#).

- [16] A. Belhaj, H. Belmahi, M. Benali and A. Segui, *Thermodynamics of AdS black holes from deflection angle formalism*, Phys. Lett. B **817** (2021) 136313.
- [17] A. Belhaj, M. Benali, A. El Balali, W. El Hadri, H. El Moumni, E. Torrente-Lujan, *Black Hole Shadows in M-theory Scenarios*, arXiv:2008.09908.
- [18] A. Belhaj, H. Belmahi, M. Benali, W. El Hadri, H. El Moumni and E. Torrente-Lujan, *Shadows of 5D Black Holes from string theory*, Phys. Lett. B **812** (2021) 136025, arXiv:2008.13478.
- [19] A. Belhaj, M. Benali, A. El Balali, H. El Moumni and S-E. Ennadifi, *Deflection angle and shadow behaviors of quintessential black holes in arbitrary dimensions*, Class. Quantum Grav. **37** (2020) 215004, arXiv:2006.01078.
- [20] J. R. Farah, D. W. Pesce, M. D. Johnson, and L. Blackburn, *On the Approximation of the Black Hole Shadow with a Simple Polar Curve*, ApJ **900** (2020) 77, arXiv:2007.06732 .
- [21] S. E. Gralla and A. Lupsasca, *Observable shape of black hole photon rings*, Phys.Rev. D (2020) 124003, arXiv:2007.10336 .
- [22] A. Belhaj, M. Benali, A. El Balali, W. El Hadri, H. El Moumni, *Shadows of Charged and Rotating Black Holes with a Cosmological Constant*, arXiv:2007.09058.
- [23] Bower G. C., et al, *The Proper Motion of the Galactic Center Pulsar Relative to Sagittarius A**, ApJ. L **2** (2014) 780, arXiv:1411.0399.
- [24] P. Kocherlakota , P. S. Joshi , S. Bhattacharyya, C. Chakraborty, A. Ray, S. Biswas, *Gravitomagnetism and Pulsar Beam Precession near a Kerr Black Hole*, MNRAS **490** (2019) 3262, arXiv:1711.04053.
- [25] R. Emparan and R. C. Myers, *Instability of superentropic black holes*. JHEP, **09** (2003)025, hep-th/0308056.
- [26] M. Appels, L. Cuspinera, R. Gregory, P. Krtous, D. Kubiznak, *Are Superentropic black holes superentropic?*. JHEP **02** (2020)195, arXiv:1911.12817.
- [27] D. Klemm, *Four-dimensional black holes with unusual horizons*, Phys.Rev. D **89** (2014) 084007, arXiv:1401.3107.
- [28] R. A. Hennigar, D. Kubiznak, and R. B. Mann, *Entropy Inequality Violations from Ultraspinning Black Holes*, Phys. Rev. Lett. **115**(2015) 031101, arXiv:1411.4309.
- [29] R A. Hennigar, D Kubiznak, R. B. Mann, N. Musoke, *Ultraspinning limits and superentropic black holes*, JHEP **096** (2015) 1506, arXiv:1504.07529.

- [30] R.A. Hennigar, D. Kubiznak and R.B. Mann, *Super-entropic black holes*, Phys. Rev. Lett. **115** (2015) 031101, [arXiv:1411.4309](#).
- [31] D. Wu, P. Wu, H. Yu, S. Q. Wu, *Notes on thermodynamics of super-entropic AdS black holes*, Phys. Rev.D **101** (2020) 024057, [arXiv:1912.03576](#).
- [32] D. Wu, S.Q. Wu, P. Wu, H. Yu, *Aspects of the dyonic Kerr-Sen-AdS black hole and its ultraspinning version*, Phys. Rev. D **103** (2021) 044014, [arXiv:2010.13518](#).
- [33] D. Wu, P. Wu, H. Yu, S. Q. Wu *Are ultra-spinning Kerr-Sen-AdS₄ black holes always super-entropic ?*, Phys. Rev. D **102** (2020) 044007, [arXiv:2007.02224](#).
- [34] S. Chandrasekhar, *The mathematical theory of black holes*, volume 69. Oxford University Press, 1998.
- [35] B. Carter, *Global structure of the kerr family of gravitational fields*. Physical Review, **174** (5) (1968)1559.
- [36] A. Grenzebach, V. Perlick, C. Lämmerzahl, *Photon Regions and Shadows of Accelerated Black Holes*, Int. J. Mod. Phys. D**24** (09) (2015) 1542024, [arXiv:1503.03036](#).
- [37] S. Haroon, M. Jamil, K. Jusufi, K. Lin, R. B. Mann, *Shadow and Deflection Angle of Rotating Black Holes in Perfect Fluid Dark Matter with a Cosmological Constant*, Phys. Rev. D **99** (12) (2019) 044015, [arXiv:1810.04103](#).
- [38] A. Grenzebach, V. Perlick, C. Lämmerzahl, *Photon Regions and Shadows of Kerr-Newman-NUT Black Holes with a Cosmological Constant*, Phys. Rev. D **89** (12) (2014) 124004, [arXiv:1403.5234](#).
- [39] Z. Hu, Z. Zhong, P.-C. Li, M. Guo, and B. Chen, *QED Effect on Black Hole Shadow*, [arXiv:2012.07022](#).
- [40] M. Wang, S. Chen, J. Wang and J. Jing, *Shadow of a Schwarzschild black hole surrounded by a Bach-Weyl ring*, Eur. Phys. J. C **80** (2020) 110, [arXiv:1904.12423](#)
- [41] H. C. D. Lima Junior, L. C. B. Crispino, P. V. P. Cunha, C. A. R. Herdeiro, *Mistaken identity: can different black holes cast the same shadow?*, [arXiv:2102.07034](#) .
- [42] C. Chen, *Rotating black holes without \mathbb{Z}_2 symmetry and their shadow images*, JCAP **05** (2020) 05, [arXiv:2004.01440](#).
- [43] M. Wang, S. Chen and J. Jing, *Shadow casted by a Konoplya-Zhidenko rotating non-Kerr black hole*, JCAP **10** (2017) 051, [arXiv:1807.00388](#).
- [44] K. Hioki, K. I. Maeda, *Measurement of the kerr spin parameter by observation of a compact object's shadow*, Phys. Rev. D, **80**(2)(2009)024042, [arXiv:0904.3575](#).

- [45] M. Amir, S. G Ghosh, *Shapes of rotating nonsingular black hole shadows*, Phys. Rev. D **94**(2) (2016) 024054, [arXiv:1603.06382](#).
- [46] R Shaikh, P. S. Joshi, *Can we distinguish black holes from naked singularities by the images of their accretion disks?*, JCAP **10** (2019) 064, [arXiv:1909.10322](#).
- [47] A. de Vries, *The apparent shape of a rotating charged black hole, closed photon orbits and the bifurcation set A_4* , Class. Quant. Grav. 17, (2000)123.
- [48] L. Amarilla, E. F. Eiroa, *Shadow of a rotating braneworld black hole*, Phys. Rev. D **85** (2012) 064019, [arXiv:1112.6349](#).